



HAL
open science

ANALYSIS AND OPTIMIZATION OF A LIQUID-VAPOR THERMOHYDRAULIC MODEL

Philippe Helluy, Gauthier Lazare

► **To cite this version:**

Philippe Helluy, Gauthier Lazare. ANALYSIS AND OPTIMIZATION OF A LIQUID-VAPOR THERMOHYDRAULIC MODEL. 2023. hal-04535413

HAL Id: hal-04535413

<https://hal.science/hal-04535413>

Preprint submitted on 6 Apr 2024

HAL is a multi-disciplinary open access archive for the deposit and dissemination of scientific research documents, whether they are published or not. The documents may come from teaching and research institutions in France or abroad, or from public or private research centers.

L'archive ouverte pluridisciplinaire **HAL**, est destinée au dépôt et à la diffusion de documents scientifiques de niveau recherche, publiés ou non, émanant des établissements d'enseignement et de recherche français ou étrangers, des laboratoires publics ou privés.

ANALYSIS AND OPTIMIZATION OF A LIQUID-VAPOR THERMOHYDRAULIC MODEL.

PHILIPPE HELLUY¹ AND GAUTHIER LAZARE²

Abstract. This work presents a simplified model of compressible multiphase fluid flow in a heated porous medium. We first introduce the model and its numerical approximation using a linearized implicit finite volume scheme. We then propose a technique to accelerate the implicit scheme through a machine learning approach.

Résumé. Ce travail présente un modèle simplifié d'écoulement de fluide multiphasique compressible dans un milieu poreux chauffant. Nous présentons d'abord le modèle et son approximation numérique par un schéma de volumes finis implicite. Nous proposons ensuite une technique d'accélération du schéma implicite par une approche d'apprentissage automatique.

1. INTRODUCTION

Very often, techniques for electricity production involve heating a heat transfer fluid (usually water). This heating is achieved through thermal exchange between the fluid and a hot medium (solar furnace, coal, gas, nuclear fuel, etc.). In order to maximize heat transfer, it is important that the heat exchange surface is large for a given volume. To achieve this, the fluid circulates in contact with a heat exchange surface, which is most often in a confined solid medium. This surface can be complex to model precisely and, for the purposes of simulation, it is convenient to assimilate the exchange area to a porous medium in which the fluid circulates. In this work, we consider a homogenized compressible model for the heat transfer fluid (water), which can locally vaporize. The two phases, due to Archimedes' force, can have different velocities. The difference in velocities is taken into account by a drift model. However, the two phases are at pressure equilibrium.

This leads to a model that is simpler to simulate numerically, but more complex mathematically. For example, it is not clear that this two-velocity, one-pressure model is hyperbolic. Many works have been conducted on this type of models, see (for example) [1, 5, 6, 11, 16] and the included references. For a general introduction to the subject of compressible multiphase fluids, we refer to [12].

The mathematical model is here approximated by a semi-implicit time-stepping scheme on a staggered grid proposed in [18]. The scheme is written in the non-conservative variables: entropy, vapor fraction, mass flow rate, and pressure. It is well suited for low Mach number flow calculations. The observed regimes do not exhibit shock waves, which justifies this choice.

Despite the simplifications adopted, obtaining the steady state from an unsteady scheme can be costly in terms of computation time, or even unstable for poor initializations or too large time steps.

The first objective of this work is to describe a model, the simplest possible, one-dimensional, but which contains most of the characteristics of the complete industrial model presented in [18]. The

¹ IRMA CNRS, Inria Tonus, Strasbourg

² EDF R&D, Chatou

second objective is to evaluate an acceleration technique, based on machine learning, for reaching the stationary solution.

2. EQUATIONS

The two-phase (water-vapor) mixture flows in a medium partially occupied by solid heating rods or tubes.

The goal of this section is to establish a system of balance laws in the form

$$\partial_t W + \nabla \cdot F(W) + \nabla \cdot (D(\nabla W)) = S(W),$$

where:

- the vector of unknowns $W(x, t)$ depends on time t and space x . This unknown vector results from mass, momentum, and energy balance equations; therefore, $W \in \mathbb{R}^3$ (homogeneous 3-equation model). The vapor mass fraction balance can also be considered to represent certain out-of-equilibrium physical phenomena, such as subcooled boiling, then $W \in \mathbb{R}^4$ (unbalanced 4-equation model),
- the flux is denoted by $F(W)$,
- the second-order flux is denoted by $D(\nabla W)$,
- the zeroth-order source term is denoted by $S(W)$.

In the following paragraphs, we detail the notations, general balance laws, and the liquid-vapor thermodynamic model. We will prioritize the zeroth and first-order terms. Second-order terms are neglected here (no solid friction, no viscosity, no heat diffusion, no turbulence). The model presented here is a simplified version of the THYC model, a two-phase thermohydraulic calculation code at the component scale, developed by EDF (see [18]).

2.1. Some Notations

Fuel rods have a complex geometry and are therefore modeled as a porous medium, as explained earlier. On a small volume V containing fluid and solid, we consider the porosity ε , defined as the ratio of the fluid volume V_f to the total volume (fluid + solid) $V = V_s + V_f$. It is a geometric parameter that depends on space x but not on time, and we always have $0 \leq \varepsilon \leq 1$. The fluid volume V_f is further decomposed into vapor volume V_v and liquid volume V_l . The two phases are immiscible, so that

$$V_f = V_l + V_v.$$

The vapor volume fraction (also called void fraction) is denoted by $\alpha = \alpha(x, t)$. It is defined as

$$\alpha = \frac{V_v}{V_l + V_v}.$$

The mixture density is defined by

$$\rho = \frac{M_l + M_v}{V_l + V_v}, \quad M_l : \text{liquid mass}, \quad M_v : \text{gas mass}.$$

Thus,

$$\rho = \alpha \rho_v + (1 - \alpha) \rho_l$$

with the densities of each phase

$$\rho_l = \frac{M_l}{V_l} \quad \text{and} \quad \rho_v = \frac{M_v}{V_v}$$

where M_l and M_v are the masses of liquid and gas, respectively. The mass fraction y (or mass fraction) of vapor is then defined as

$$y = \frac{\alpha \rho_v}{\rho} = \frac{M_v}{M_l + M_v} \quad \text{and} \quad 1 - y = \frac{(1 - \alpha)}{\rho} \rho_l. \quad (1)$$

We also define the volumetric momentum q of the mixture

$$q = \frac{M_v u_v + M_l u_l}{V_v + V_l} = \rho u,$$

which defines the mixture velocity u from the velocities of each phase u_l and u_v . We also define u_r , the relative velocity between the two phases

$$u_r = u_v - u_l.$$

From these relations, we deduce the following relationships

$$\begin{aligned} \rho u &= \alpha_l \rho_l u_l + \alpha_v \rho_v u_v, \\ u_l &= u - y u_r, \quad u_v = u + (1 - y) u_r. \end{aligned} \quad (2)$$

Surface tension is neglected, and we consider pressure equilibrium between the phases, i.e., $p = p_v = p_l$. We define the specific internal energy of the mixture e and the specific enthalpy of the mixture $h = e + \frac{p}{\rho}$ from the specific internal energy and specific enthalpy of each phase

$$e = y e_v + (1 - y) e_l,$$

$$h = y h_v + (1 - y) h_l.$$

Finally, we also define the enthalpy difference

$$L = h_v - h_l. \quad (3)$$

2.2. Balance laws

In this section, each balance law is derived from principles of mechanics. We use the approach of [15], which has the advantage of being particularly concise. For each balance, we consider a fixed domain Ω in space. The outward unit normal to Ω on $\partial\Omega$ is denoted by n .

2.2.1. Mass balance

The conservation of total mass is written in the same way for both the multiphase model and a compressible single-fluid model:

$$\partial_t(\varepsilon\rho) + \nabla \cdot (\varepsilon q) = 0. \quad (4)$$

Using the method of [15], during a time dt , the mass of phase k crossing an element of surface ds is given by $\varepsilon \alpha_k \rho_k u_k \cdot n ds dt$. This leads to the equation

$$\frac{d}{dt} \int_{\Omega} \varepsilon \rho = - \int_{\partial\Omega} (\varepsilon \alpha_l \rho_l u_l \cdot n + \varepsilon \alpha_v \rho_v u_v \cdot n) = \int_{\partial\Omega} \varepsilon \rho u \cdot n,$$

which indeed gives (4), thanks to the Stokes formula.

2.2.2. Momentum balance

The momentum balance is more complex as it must take into account the relative velocity between the two phases, which is not *a priori* zero. The equation is written as

$$\partial_t(\varepsilon q) + \nabla \cdot (\varepsilon \rho u \otimes u + \varepsilon p I) + \nabla \cdot (\varepsilon \rho y (1 - y) u_r \otimes u_r) = \varepsilon \rho g + I_{fs} + I_t \quad (5)$$

where g is the acceleration due to gravity, I_t is turbulent dissipation, and I_{fs} is dissipation due to head loss (corresponding to friction between the solid and the fluid). As mentioned earlier, friction is neglected here, so $I_t = 0$ and $I_{fs} = 0$.

The equation (5) then becomes

$$\partial_t(\varepsilon q) + \nabla \cdot (\varepsilon \rho u \otimes u + \varepsilon p I) + \nabla \cdot (\varepsilon \rho y (1 - y) u_r \otimes u_r) = \varepsilon \rho g. \quad (6)$$

To establish this conservation equation, we can also reason as in [15]. The change in momentum in the domain Ω is equal to the sum of the momentum crossing the boundary by convection, the pressure forces (neglecting surface tension), acting on the boundary, and the volumetric forces. We find

$$\begin{aligned} \frac{d}{dt} \int_{\Omega} \varepsilon \rho u &= - \int_{\partial\Omega} \varepsilon \alpha_l \rho_l u_l u_l \cdot n + \varepsilon \alpha_v \rho_v u_v u_v \cdot n \\ &\quad - \int_{\partial\Omega} \varepsilon p n \\ &\quad + \int_{\Omega} \varepsilon \rho g. \end{aligned}$$

Using the relations (1), we obtain

$$\begin{aligned} \frac{d}{dt} \int_{\Omega} \varepsilon \rho u &= - \int_{\partial\Omega} (\varepsilon(1-y)\rho u_l u_l \cdot n + \varepsilon y \rho u_v u_v \cdot n) \\ &\quad - \int_{\partial\Omega} \varepsilon p n \\ &\quad + \int_{\Omega} \varepsilon \rho g. \end{aligned}$$

We then use the relations (2) and the Stokes formula to conclude.

2.2.3. Energy balance

For the energy balance, several terms need to be considered to account for the relative velocity and the latent heat of vaporization. We start by establishing the conservative formulation of the energy balance. For this, we introduce the total specific energy of each phase k

$$\eta_k = e_k + \frac{u_k^2}{2}.$$

The total specific energy of the mixture is then given by

$$\begin{aligned} \rho \eta &= \sum_k \alpha_k \rho_k e_k + \alpha_k \rho_k \frac{u_k^2}{2}, \\ \eta &= y e_v + (1-y) e_l + y \frac{u_v^2}{2} + (1-y) \frac{u_l^2}{2}. \end{aligned}$$

Using the relations (2), the total energy can be rewritten as

$$\eta = y e_v + (1-y) e_l + \frac{u^2}{2} + y(1-y) \frac{u_r^2}{2}.$$

Note that we do not have the equality $\eta = e + \frac{u^2}{2}$ in the case where the relative velocity is non-zero. When writing the energy balance, we still use the technique presented in [15]. The temporal variation of energy in Ω

$$\frac{d}{dt} \int_{\Omega} \varepsilon \rho \eta$$

is given by the balance of several terms:

- the quantity of energy that crosses the boundary by convection

$$W_1 = - \int_{\partial\Omega} (\varepsilon \alpha_l \rho_l \eta_l u_l \cdot n + \varepsilon \alpha_v \rho_v \eta_v u_v \cdot n),$$

- the work of the pressure force at the boundary

$$W_2 = - \int_{\partial\Omega} (\varepsilon \alpha_l p u_l \cdot n + \varepsilon \alpha_v p u_v \cdot n),$$

- the work of the forces in the volume

$$W_3 = \int_{\Omega} \varepsilon \rho g \cdot u,$$

- heat sources, with ϕ the heat source from the solid, ϕ_{dif} the diffusion heat flux and ϕ_t the turbulent heat flux

$$W_4 = \int_{\Omega} \phi + \int_{\partial\Omega} \varepsilon (\phi_{dif} + \phi_t) \cdot n.$$

After calculations, the terms W_i can be simplified. For W_1 one finds

$$\begin{aligned} W_1 &= - \int_{\partial\Omega} \varepsilon \rho \eta u \cdot n \\ &\quad - \int_{\partial\Omega} \varepsilon \rho y (1 - y) (\eta_v - \eta_l) u_r \cdot n, \end{aligned}$$

For W_2

$$W_2 = - \int_{\partial\Omega} \varepsilon p u \cdot n = - \int_{\partial\Omega} \varepsilon p (\alpha - y) u_r \cdot n.$$

One can also write (after calculations)

$$W_2 = - \int_{\partial\Omega} \varepsilon p u \cdot n = - \int_{\partial\Omega} \varepsilon p \rho y (1 - y) (\tau_v - \tau_l) u_r \cdot n.$$

The conservative form of the equations is therefore

$$\begin{aligned} &\partial_t \varepsilon \rho \eta + \nabla \cdot (\varepsilon (\rho \eta + p) u) \\ &\quad + \nabla \cdot (\varepsilon \rho y (1 - y) (\eta_v + \tau_v p - (\eta_l + \tau_l p)) u_r) \\ &= \varepsilon \rho g \cdot u + \phi + \nabla \cdot \varepsilon (\phi_t + \phi_{dif}). \end{aligned}$$

Since in this work we neglect terms of order 2, $\phi_t + \phi_{dif} = 0$

To obtain the equation for internal energy only, one must write the kinetic energy equation and the equation for the quantity $y(1 - y) \frac{u_r^2}{2}$ and subtract them from the total energy equation.

The kinetic energy equation is obtained by multiplying the momentum equation (6) by u and using the mass conservation equation (4)

$$\partial_t (\varepsilon \rho \frac{u^2}{2}) + \nabla \cdot \left(\varepsilon \rho u \frac{u^2}{2} \right) + \varepsilon u \cdot \nabla p + u \cdot (\nabla \cdot (\varepsilon \rho y (1 - y) u_r^2)) = \varepsilon \rho g \cdot u.$$

For the equation on the quantity $y(1 - y) \frac{u_r^2}{2}$, the momentum equation for the vapor phase is multiplied by $(1 - y) u_r$ and that for the liquid phase by $y u_r$. The vapor phase equation is then subtracted from that of the liquid phase, and the equation for the mass balance of the vapor is added, multiplied by the quantity $(1 - 2y) \frac{u_r^2}{2}$. The final result is the equation for the quantity $y(1 - y) \frac{u_r^2}{2}$

$$\begin{aligned} &\partial_t (\varepsilon \rho y (1 - y) \frac{u_r^2}{2}) + \nabla \cdot \left(\varepsilon \rho y (1 - y) u_r \frac{u_r^2}{2} \right) + (\rho y (1 - y) \varepsilon \frac{u_r^2}{2} \partial_x u + \partial_x (\rho y (1 - y) \varepsilon u_r (1 - 2y) \frac{u_r^2}{2})) = \\ &\quad - \rho y (1 - y) (\tau_v - \tau_l) \varepsilon \partial_x p - p u_r \varepsilon \partial_x \alpha + I_p u_r - \Gamma \left(\frac{u_g^2}{2} - \frac{u_l^2}{2} \right) \end{aligned}$$

with I_p the momentum exchange term between the vapor phase and the liquid phase and Γ the mass exchange term between the vapor phase and the liquid phase. After calculations, one finally obtains the following internal energy equation

$$\begin{aligned} \partial_t \varepsilon \rho e + \nabla \cdot (\varepsilon \rho u e) + \varepsilon (pI + \rho y (1 - y) u_r^2) \cdot \nabla u + \nabla \cdot (\varepsilon \rho y (1 - y) (h_v - h_l) u_r) = \\ \phi + \left(\Gamma \left(\frac{u_g^2}{2} - \frac{u_l^2}{2} \right) - u_r I \right) + p u_r \varepsilon \partial_x \alpha. \end{aligned} \quad (7)$$

In the applications considered, the heat flux is very large, which allows us to neglect the terms on the right-hand side of the equation $(\Gamma(\frac{u_g^2}{2} - \frac{u_l^2}{2}) - u_r I) + p u_r \varepsilon \partial_x \alpha$. Using the formula $h = e + p\tau$, the enthalpy balance of the mixture becomes

$$\begin{aligned} \partial_t (\varepsilon \rho h - \varepsilon p) + \nabla \cdot (\varepsilon h q) + \nabla \cdot (\varepsilon \rho y (1 - y) L u_r) = \\ \varepsilon \left(u + y (1 - y) \rho \left(\frac{1}{\rho_v} - \frac{1}{\rho_l} \right) u_r \right) \cdot \nabla p + \phi. \end{aligned} \quad (8)$$

The enthalpy gap L is given by equation (3). For our application, we can approximate the heating term ϕ as a constant, in a first approximation.

2.2.4. Mass Balance of Gases

In the case where the mixture is not at thermodynamic equilibrium, the temperature of the liquid can be, on average, lower than the saturation temperature, while observing steam production. This is explained by the fact that the saturation temperature is reached locally. This phenomenon is called unsaturated boiling. In this case, the fourth equation translates the mass balance of the steam

$$\partial_t (\varepsilon \rho y) + \nabla \cdot (\varepsilon y q) + \nabla \cdot (\varepsilon y (1 - y) \rho u_r) = \Gamma, \quad (9)$$

where Γ the production term is divided into two terms

$$\Gamma = \Gamma_\phi + \Gamma_p,$$

with Γ_ϕ the steam production due to heat flow (direct steam production) and Γ_p the steam production by pressure effect (return to thermodynamic equilibrium term). We introduce this equation for completeness and because we will need to take into account these terms in future works. However, in the numerical simulations of this article, steam is always assumed to be at equilibrium. Equation (9) will therefore not be taken into account. The mass fraction is always taken at equilibrium y_{eq} .

2.3. Modeling

The equations proposed previously are based, as a whole, on fundamental principles: geometric transport, conservation, Newton's laws, thermodynamics. The task now is to propose a thermodynamic model for the two-phase liquid-vapor mixture. In addition, the relative velocity must be modeled by a correlation to close the equations.

2.3.1. Thermodynamics of the Mixture

We assume that the complete equations of state of the liquid and vapor are known. Examples of these equations of state, based on stiffened gases, are given in Appendix 1. There are several ways to write these complete equations of state, for example, we can give the specific energy of each phase k . For each phase k , the specific energy e_k is a function of the specific volume $\tau_k = \frac{1}{\rho_k}$ and the specific entropy s_k

$$e_k = e_k(\tau_k, s_k).$$

All other thermodynamic variables can be obtained from e_k

- temperature

$$\theta_k = \frac{\partial}{\partial s_k} e_k(\tau_k, s_k),$$

- pressure

$$p_k = - \frac{\partial}{\partial \tau_k} e_k(\tau_k, s_k), \quad (10)$$

- chemical potential

$$\mu_k = e_k + p_k \tau_k - \theta_k s_k,$$

- enthalpy

$$h_k = e_k + p_k \tau_k.$$

Using the state equations of each phase, we can establish a state equation for the mixture, which is consistent with thermodynamic laws. For this, we start by defining the mass energy of the mixture with the formula

$$e = y e_v(\tau_v, s_v) + (1 - y) e_\ell(\tau_\ell, s_\ell).$$

But also $\tau_k = \frac{V_k}{M_k} = \frac{V_k}{V} \cdot \frac{V}{M} \cdot \frac{M}{M_k}$. So

$$\tau_v = \frac{\alpha}{y} \tau, \quad \tau_\ell = \frac{1 - \alpha}{1 - y} \tau.$$

Similarly

$$s_v = \frac{z}{y} s, \quad s_\ell = \frac{1 - z}{1 - y} s, \quad (11)$$

where z is the entropy fraction of the vapor. So

$$e = y e_v\left(\frac{\alpha}{y} \tau, \frac{z}{y} s\right) + (1 - y) e_\ell\left(\frac{1 - \alpha}{1 - y} \tau, \frac{1 - z}{1 - y} s\right). \quad (12)$$

For a more detailed discussion of this choice, see (for example) [2, 3, 7, 8]. *A priori*, the energy of the mixture is a function of (τ, s, y, z, α) . However, certain equilibria will allow the elimination of the volume fraction α and the entropy fraction z . The equilibrium is determined by maximizing the energy. Let's calculate the differential of e

$$\begin{aligned} de &= -(\alpha p_v + (1 - \alpha) p_\ell) d\tau \\ &\quad + (z \theta_v + (1 - z) \theta_\ell) ds \\ &\quad + (\mu_v - \mu_\ell) dy \\ &\quad + s(\theta_v - \theta_\ell) dz \\ &\quad - \tau(p_v - p_\ell) d\alpha. \end{aligned} \quad (13)$$

As explained in Section 2.2.4, we give details of the calculations in the non-equilibrium case, with sub-saturated boiling, for the sake of completeness. However, in the numerical results, we will assume that the vapor is in equilibrium.

Mechanical Equilibrium. To obtain mechanical equilibrium, we maximize the mixing energy with respect to the volume fraction α . From equation (13), this results in pressure equilibrium between the two phases:

$$p = p_v = p_\ell.$$

Thermal Equilibrium. Similarly, the thermal equilibrium condition can be established by maximizing energy with respect to the entropy fraction z . Thermal equilibrium is achieved when the temperatures of both phases are equal:

$$\theta_v = \theta_\ell.$$

However, assuming thermal equilibrium is not realistic in the mean model when considering the unbalanced model with 4 equations. This assumption is true in the 3-equation model, where both phases are at the same temperature, the saturation temperature.

Chemical Equilibrium: We assume that any locally appearing vapor is in chemical equilibrium with the surrounding liquid:

$$\mu_v(p, \theta_v) = \mu_\ell(p, \theta_*),$$

where θ_* is the temperature of the liquid in immediate contact with the vapor. In general, vapor appears near heat-emitting solids. However, a control volume may encompass a larger area where the liquid temperature is not saturated on average.

A more realistic assumption is that there is local thermal equilibrium between the vapor and the liquid in direct contact with the vapor. In this case, the vapor remains saturated (no superheating), and

$$\theta_* = \theta_v.$$

This leads to

$$\mu_v(p, \theta_v) = \mu_\ell(p, \theta_v). \quad (14)$$

This is the definition of the saturation temperature:

$$\mu_v(p, \theta_{sat}) = \mu_\ell(p, \theta_{sat}).$$

The chemical equilibrium can also be expressed as

$$\theta_v = \theta_{sat}(p) = \theta_v(p). \quad (15)$$

This eliminates the entropy fraction z from the calculations. From equation (11), we have

$$z = \frac{y s_v(p)}{s}.$$

Given the saturation condition (15), the vapor entropy only depends on the pressure. This results in

$$dz = \frac{s_v}{s} dy + \frac{y}{s} s'_v(p) dp - \frac{y s_v}{s^2} ds, \quad (16)$$

where $s'_v(p)$ is the derivative of the vapor entropy with respect to the pressure.

Energy Balance. To summarize the previous calculations, the differential of the mixing energy (13) can be rewritten as:

$$\begin{aligned} de &= -pd\tau \\ &+ (z\theta_v(p) + (1-z)\theta_\ell) ds \\ &+ (\mu_v(p, \theta_v(p)) - \mu_\ell(p, \theta_\ell)) dy \\ &+ (\theta_v(p) - \theta_\ell) s dz. \end{aligned}$$

With (16), $z = y s_v / s$, we obtain

$$\begin{aligned} de &= -pd\tau \\ &+ (z\theta_v(p) + (1-z)\theta_\ell) ds \\ &+ (\mu_v(p, \theta_v(p)) - \mu_\ell(p, \theta_\ell)) dy \\ &+ (\theta_v(p) - \theta_\ell) (s_v dy + y s'_v(p) dp - z ds). \end{aligned}$$

Switching to enthalpy $h = e + p\tau$ we get

$$\begin{aligned} dh &= (\tau + y(\theta_v(p) - \theta_\ell) s'_v(p)) dp \\ &+ \theta_\ell ds \\ &+ ((\theta_v(p) - \theta_\ell) s_v + \mu_v(p, \theta_v(p)) - \mu_\ell(p, \theta_\ell)) dy, \end{aligned} \quad (17)$$

which gives

$$\begin{aligned} dh &= (\tau + y(\theta_v(p) - \theta_\ell) s'_v(p)) dp \\ &+ \theta_\ell ds \\ &+ (h_v - h_\ell + \theta_\ell(s_\ell - s_v)) dy. \end{aligned} \quad (18)$$

Recalling that

$$L = h_v - h_\ell,$$

and defining

$$\bar{L} = s_v(p) - s_\ell,$$

we also have

$$\begin{aligned} dh &= (\tau + y(\theta_v(p) - \theta_\ell)s'_v(p)) dp \\ &\quad + \theta_\ell ds \\ &\quad + (L - \theta_\ell \bar{L}) dy. \end{aligned} \tag{19}$$

Thermal Imbalance: As explained above, we do not always assume thermal equilibrium. In the chosen model, generally,

$$\theta_\ell \neq \theta_v.$$

This thermal imbalance has consequences for the calculation of the mixture variables. In particular, since $\partial_s h = \theta$, we see from equation (17) that the constraint $\theta_v = \theta_{sat}(p)$ imposes that the temperature of the mixture is the temperature of the liquid

$$\theta = \theta_\ell. \tag{20}$$

Calculation of other variables. The numerical model will be resolved in the following variables: flow rate, entropy, pressure, and concentration, (q, s, p, y) . Therefore, we need to know how to calculate all other thermodynamic variables from y, s, p . We know that

$$s = ys_v + (1 - y)s_\ell$$

where s_ℓ and s_v denote the specific entropy of the liquid and vapor, respectively. The vapor is always saturated, so

$$\theta_v = \theta_{sat}(p).$$

We can then deduce the specific entropy of the vapor (here expressed as a function of pressure and temperature)

$$s_v = s_v(\theta_v, p),$$

which gives us s_ℓ

$$\begin{aligned} s_\ell &= \frac{s - ys_v}{1 - y} \text{ if } y < 1, \\ &= 0 \text{ otherwise. This regime is never encountered in practice.} \end{aligned}$$

We can then deduce all other thermodynamic quantities for the liquid, since we know two variables (here the pressure p and entropy s_ℓ).

Relative Velocity. The relative velocity must be modeled by a closure law to obtain a closed system of equations. It is decomposed into two terms

$$u_r = v_r - \frac{D}{y(1 - y)} \nabla y.$$

The gradient of concentration term is related to turbulent diffusion. The diffusion coefficient D is often given by a model, but this second-order term is neglected in this article. The drift-flux term v_r along the vertical axis is taken from the correlation of Bestion (initially developed for the CATHARE software, see for example [4])

$$v_r = 0.188 \frac{1 + y(\delta - 1)}{1 - y} \sqrt{gd_h(\delta - 1)},$$

where d_h is a characteristic length, depending on the geometry of the solid, and

$$\delta = \frac{\rho_l}{\rho_v}.$$

2.4. Vectorial Formulation

We can gather the equations into a system of conservation laws of the form

$$\partial_t W + \nabla \cdot Q(W, x) = S(W).$$

The vector of conservative variables is

$$W = \begin{pmatrix} \varepsilon \rho \\ \varepsilon q \\ \varepsilon \rho \eta \\ \varepsilon \rho y \end{pmatrix}.$$

The flux Q contains the first-order terms in W . We have

$$Q(W) \cdot n = \begin{pmatrix} \varepsilon q \cdot n \\ \varepsilon (q \cdot nu + pn + \rho y(1-y)u_r \cdot nu_r) \\ \varepsilon (q \cdot n\eta + pu \cdot n + \rho y(1-y)(\eta_v + \tau_v p - (\eta_l + \tau_l p))u_r \cdot n) \\ \varepsilon y q \cdot n + \varepsilon \rho y(1-y)u_r \cdot n \end{pmatrix},$$

and

$$S(W) = \begin{pmatrix} 0 \\ \varepsilon \rho g \\ \phi \\ \Gamma_p + \Gamma_\phi \end{pmatrix}.$$

3. PRIMITIVE FORMULATION OF THE EQUATIONS

The objective is to obtain a primitive formulation for the four equations with more physical unknowns: pressure, flow rate, entropy, and concentration (p, q, s, y) . It is this non-conservative formulation which will be used numerically. The considered applications do not exhibit shocks. Therefore, there is no particular difficulty related to the definition of the Rankine-Hugoniot jump relations.

3.1. Pressure Equation

The differential of the density with respect to the variables (p, q, s) is given by:

$$d\rho = \frac{1}{c_s^2} dp + \beta ds + \gamma dy, \quad (21)$$

where the expressions of the coefficients $\frac{1}{c_s^2}, \beta$ and γ are detailed in Appendix 1. In the case where a homogeneous model with 3 equations is considered, that is, when the vapor concentration is always at equilibrium, $y = y^{eq}$, we have $\gamma = 0$.

Using the differential on the mass conservation equation (4) and recalling that the porosity ε does not depend on time, the pressure equation becomes

$$\varepsilon \partial_t p + c_s^2 \nabla \cdot (\varepsilon q) = -\varepsilon \beta c_s^2 \partial_t s - \varepsilon \gamma c_s^2 \partial_t y \quad (22)$$

3.2. Entropy Equation

Using the differential of enthalpy (19), we can deduce a simple expression for the differential of entropy for the homogeneous model. In fact, in this case, saturation is reached $\theta_l = \theta_v = \theta_{sat}$ and then

$$\theta_l ds = dh - \tau dp.$$

The saturation hypothesis also allows us to write

$$L = \theta_l \bar{L}$$

and

$$\theta_l d\bar{L} = dL - (\tau_v - \tau_l) dp.$$

Rewriting the energy equation in non-conservative form (using mass conservation)

$$\rho\varepsilon(\partial_t h - \tau\partial_t p + u \cdot (\nabla h - \tau\nabla p)) + \rho\varepsilon y(1-y)u_r \cdot (\nabla L - (\tau_v - \tau_l)\nabla p) + L\nabla \cdot (\varepsilon\rho y(1-y)u_r) = \phi,$$

and using the previous differentials, the entropy equation is

$$\theta_l(\varepsilon\rho\partial_t s + \varepsilon\rho u \cdot \nabla s + \nabla \cdot (\varepsilon\rho y(1-y)u_r \bar{L})) = \phi. \quad (23)$$

This equation also has a conservative form

$$\partial(\varepsilon\rho s) + \nabla \cdot (\varepsilon\rho u s + \varepsilon\rho y(1-y)u_r \bar{L}) = \frac{\phi}{\theta_l}. \quad (24)$$

3.3. Final Equation System

The conservation equations for momentum and the mass vapor title are also written in primitive form. The final model is

$$\varepsilon\rho\partial_t s + \varepsilon q \cdot \nabla s + \nabla \cdot (\varepsilon\rho y(1-y)u_r \bar{L}) = \frac{\phi}{\theta_l}, \quad (25)$$

$$\varepsilon\rho\partial_t y + \varepsilon q \cdot \nabla y + \nabla \cdot (\varepsilon\rho y(1-y)u_r) = \Gamma_p + \Gamma_\phi, \quad (26)$$

$$\varepsilon\partial_t p + c_s^2 \nabla \cdot (\varepsilon q) = -\varepsilon\beta c_s^2 \partial_t s - \varepsilon\gamma c_s^2 \partial_t y, \quad (27)$$

$$\varepsilon\partial_t q + \nabla \cdot (\varepsilon u \otimes q) + \nabla(\varepsilon p) + \nabla(\varepsilon\rho y(1-y)u_r \otimes u_r) = \varepsilon\rho g. \quad (28)$$

Note: Non-conservative terms $\varepsilon q \cdot \nabla f$ are treated numerically by separating them into two parts such that $\varepsilon q \cdot \nabla f = \nabla \cdot (\varepsilon f q) - f \nabla \cdot (\varepsilon q)$.

4. NUMERICAL RESOLUTION

In this section, we describe the ThermoTorch code developed to approach the previously described two-phase model on a one-dimensional domain.

4.1. Resolution Method

The resolution algorithm for a time step proceeds as follows:

- (1) Thermodynamic variables are updated from the fields (p, s) (or (p, s, y) in the 4-equation model) obtained from the previous time step. During this step, the equilibrium thermodynamic concentration y^{eq} is also evaluated.
- (2) The entropy equation (25) is solved. The only implicit variable in this step is the entropy. The equation becomes independent of the other unknowns and can be treated alone. Moreover, this implicit system is a linear system.
- (3) *Only for the 4-equation model:* The concentration equation (26) is solved. This step simplifies for the homogeneous 3-equation model since the concentration is at equilibrium $y = y^{eq}$.
- (4) The coupled pressure-momentum system (p, q) (27-28) is solved. The flow and pressure are calculated by an implicit scheme. The entropy and concentration obtained in steps 3 and 4 are taken explicitly in the pressure equation.

4.2. Numerical Scheme

4.2.1. Discretization

The resolution is carried out using a 1D staggered grid scheme, which consists of a grid for the pressure p , entropy s , and concentration y and a second grid for the flow q . This choice is justified by the fact that this type of scheme has good behavior in the low Mach limit (see for example [9]). For this, we consider a mesh of the interval $[0, L]$ with cells C_i , $0 \leq i < N + 1$. The mesh size is constant and equal to

$$\Delta x = \frac{2L}{2N - 1}$$

and the cells are then

$$C_i =](i - 1)\Delta x, i\Delta x[.$$

We denote by p_i the pressure at the center of the cell C_i , at the point $x_i = (i - \frac{1}{2})\Delta x$, $0 \leq i < N + 1$. The same convention is used for entropy s_i and concentration y_i . The notation $q_{i-1/2}$ is used for the flow at the edges of the cells, at the points $x_{i-1/2} = (i - 1)\Delta x$, $1 \leq i < N + 1$. The flow is assumed to occur from left to right, i.e., $q_{i-1/2} > 0, \forall i$.

Cell C_0 is used to impose the entropy boundary condition (it is called a ghost cell) at the entrance of the domain. The following value is fixed

$$s_0 = s_{in}.$$

For the 4-equation model, the boundary condition for concentration is also added. The inlet flow rate is imposed on the first cell C_1 with

$$q_{1/2} = q_{in}$$

The cell C_N allows to impose the boundary condition for the pressure outlet:

$$p_N = p_{out}$$

A constant heat flow is imposed in the domain $[\frac{L}{8}, \frac{7L}{8}]$:

$$\phi(x \in [\frac{L}{8}, \frac{7L}{8}]) = \phi_0, \quad \phi(x) = 0 \text{ otherwise.}$$

Remark: For each calculation, the only input parameters are therefore $(\theta_{in}, q_{in}, p_{out}, \phi_0)$ for the 3-equation model. This reduced number of parameters will allow to predict the solution using a very simple neural network.

4.2.2. Numerical Schemes

In the following, we denote by λ the ratio of the time step Δt and the grid step Δx

$$\lambda = \frac{\Delta t}{\Delta x}.$$

For the entropy and flow equation, convection is treated by a centered scheme considering a positive flow rate. We consider all known quantities at time step n . The typical finite volume discretization of the equations allows to obtain the unknowns at time step $n + 1$.

The discretization of the vapor fraction equation is not detailed here. We consider only the 3-equation model in the presented numerical applications. Moreover, in the considered framework, we assume that the porosity is constant and that the relative velocity is zero.

4.3. Discretization of the entropy equation

The discretization of entropy for cell i is written by freezing all quantities at time step n (including the flow rate) except entropy to obtain a linear system

$$a_i^s s_i^{n+1} + m_i^s s_{i-1}^{n+1} = b_i^s,$$

with

$$\begin{aligned} a_i^s &= 1 + \frac{\lambda}{\rho_i^n} q_{i-1/2}^n, \\ m_i^s &= -\frac{\lambda}{\rho_i^n} q_{i-1/2}^n, \\ b_i^s &= s_i^n + \frac{\phi_i^n \Delta t}{\rho_i^n \theta_{l,i}^n}. \end{aligned}$$

4.4. Discretization of the coupled pressure-flow system

The pressure and flow equations are resolved in a coupled manner. For the pressure equation, the entropy increment (and vapor fraction for the 4 equations model) is necessary. It is determined by solving the independently presented entropy equation. For the flow equation, the convection velocity is frozen at time step n to obtain a linear system. The pressure grid $u_{p,i}$ is necessary in the flow equation. It is determined by the formula

$$u_{p,i}^n = \frac{q_{i-1/2}^n + q_{i+1/2}^n}{2\rho_i^n}$$

The linear system is written

$$\begin{aligned} p_i^{n+1} + \lambda(c_{s,i}^n)^2 (q_{i+1}^{n+1} - q_i^{n+1}) &= p_i^n - \beta_i^n (c_{s,i}^n)^2 (s_i^{n+1} - s_i^n) - \gamma_i^n (c_{s,i}^n)^2 (y_i^{n+1} - y_i^n), \\ (1 + \lambda u_{p,i+1}^n) q_{i+1/2}^{n+1} - \lambda u_{p,i}^n q_{i-1/2}^{n+1} + \lambda (p_{i+1}^{n+1} - p_i^{n+1}) &= q_{i+1/2}^n. \end{aligned}$$

5. NUMERICAL APPLICATIONS

5.1. Simplified Test Case

In order to validate the implementation of the code, we consider an analytical stationary solution of the equations (25-26-27-28). The method of calculation of this solution is given in [10]. We consider here the homogeneous model with 3 equations and no relative velocity. The vapor phase is therefore at saturation.

This solution is evaluated for two typical cases: case (1) of monophasic calculation (high flow rate) and case (2) of two-phase calculation (low flow rate). The physical parameters retained for the two cases are summarized in Table 1. The length of the domain is fixed at $L = 4.6\text{m}$.

param.	cas (1)	cas (2)	unit
inlet flow rate q_{in}	3500	1500	kg/s
inlet temperature θ_{in}	320	320	$^{\circ}C$
outlet pressure p_{out}	155	155	bar
imposed heat flow ϕ_0	10^8	10^8	$J/s/m^3$

TABLE 1. Numerical parameters for the test cases (1) and (2).

In Figure 1 (resp. 2), we represent the spatial variations of the stationary state (mass density, pressure, temperature, quality) in case (1) (resp. (2)). We observe the good correspondence between the numerical solution and the analytical solution. In Figure 3, we observe the convergence of the

numerical method towards the analytical solution for the two cases considered. The convergence is of order one as expected.

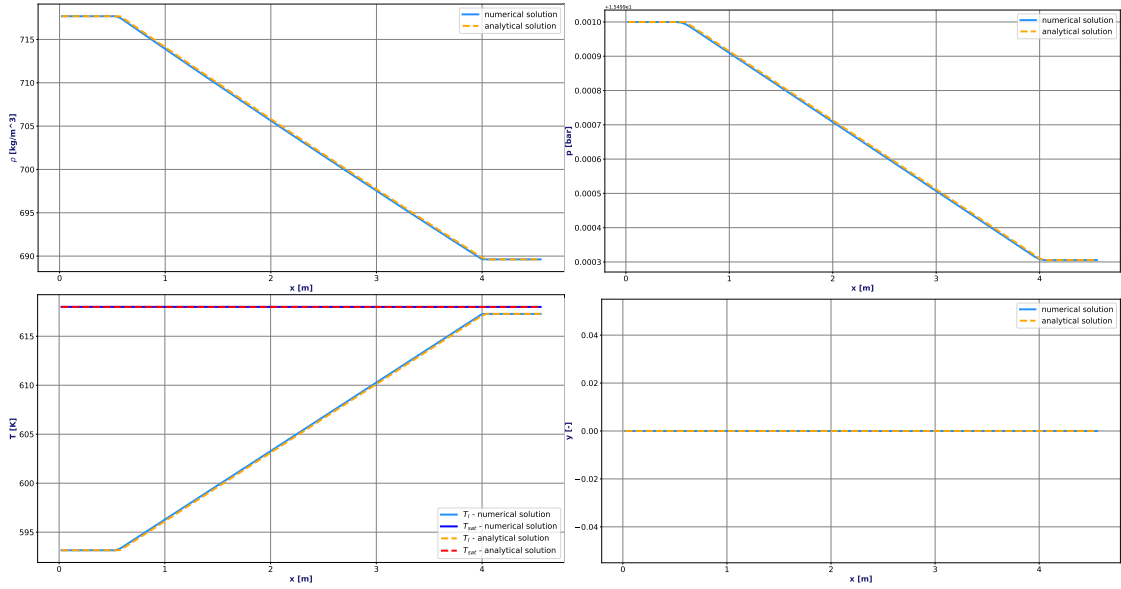


FIGURE 1. From left to right and top to bottom: mass density, pressure, temperature and vapor fraction for the stationary state of case (1). The numerical solution (solid line) is compared with the analytical solution (dashed line) for a mesh of size $N = 100$.

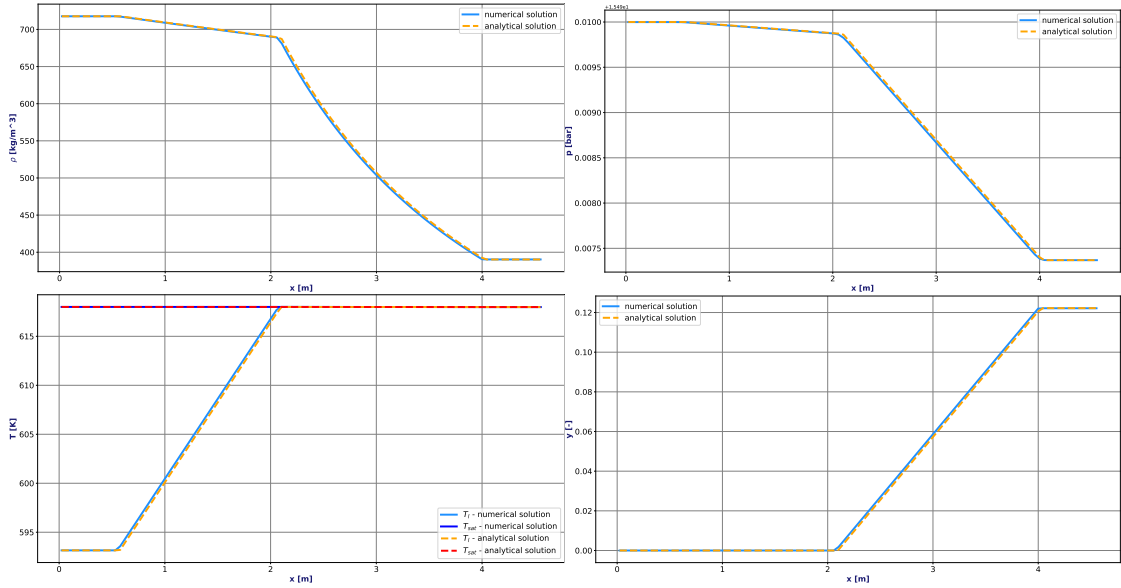


FIGURE 2. From left to right and top to bottom: mass density, pressure, temperature and vapor fraction for the stationary state of case (2). The numerical solution (solid line) is compared with the analytical solution (dashed line) for a mesh of size $N = 100$.

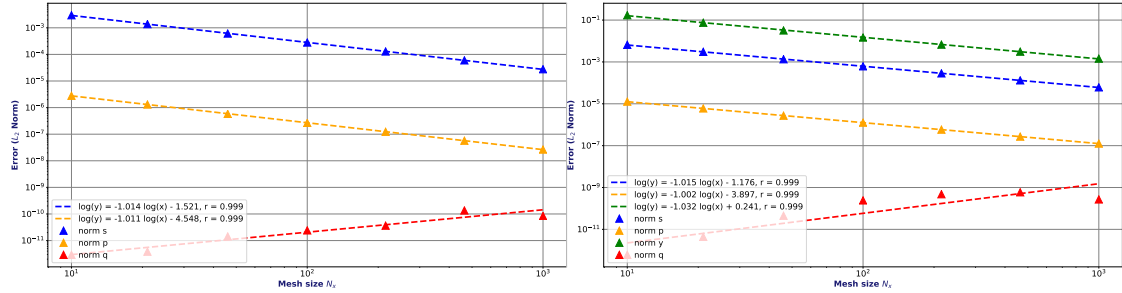


FIGURE 3. Convergence test of the scheme for test cases (1) (left) and (2) (right) - residuals for different variables: pressure, flow rate, entropy and vapor fraction (if two-phase).

6. MOTIVATION

In order to reach the stationary state, we solve the unsteady flow by starting from an initial state. If this initial state is arbitrary (for example a uniform state), the convergence towards the stationary state can be costly in terms of computation time. Furthermore, the calculation may not converge, or may require significant reductions in the time step Δt to avoid the appearance of non-physical values.

The current initialization (model with 3 equations) of ThermoTorch consists of initializing the solution fields (p, s, q) from constant properties of the unsaturated liquid water:

$$p(x, t = 0) = p_{out} \quad ; \quad s(x, t = 0) = s_l(p_{out}, \theta_{in}) \quad ; \quad q(x, t = 0) = q_{in}.$$

A fictitious unsteady simulation is used to reach the stationary solution $(\bar{p}, \bar{s}, \bar{q})$. This unsteady computations require N_{iter}^{ic} iterations when the fields are initialized by constant fields for reaching the stationary state up to a given precision.

In order to accelerate convergence, we will train a neural network to predict the stationary solution from input parameters $(q_{in}, \theta_{in}, \phi, p_{out})$. We will use this prediction (p^{ml}, s^{ml}) as initialization for the ThermoTorch simulation. The prediction can then be written

$$p^{ml}(x) = \bar{p}(x) + \nu_p(x)\Delta p,$$

$$s^{ml}(x) = \bar{s}(x) + \nu_s(x)\Delta s$$

with $\Delta p = \max_x(\bar{p}(x) - p_{out})$ and $\Delta s = \max_x(\bar{s}(x) - s_l(p_{out}, \theta_{in}))$. The functions ν_s and ν_p are functions evaluating the error made by the prediction compared to the stationary solution. If we denote N_{it}^{ML} the number of iterations necessary to reach convergence with this prediction as initialization, the goal is to make the neural network predict the solution with small enough errors ν_p and ν_s to obtain $N_{it}^{ML} < N_{it}^{ic}$.

Note: In this simple 1D case, the flow rate is not yet used, as the stationary solution is constant ($\bar{q}(x) = q_{in}$).

In order to validate the concept and evaluate the errors (ν_s, ν_p) necessary for significant acceleration, a test case is carried out with a randomly generated perturbation of the form

$$\nu_{s,p}(x) = P_{s,p}(x)\bar{\nu}$$

where $P_s(x)$ and $P_p(x)$ are random variables following a uniform law on the interval $[-1,1]$ and $\bar{\nu}$ is a constant defining the amplitude of the perturbation.

The test cases in Table 1 are used again. The single-phase test case (1) requires $N_{it}^{ic} = 31$ iterations before convergence and the two-phase test case (2) requires $N_{it}^{ic} = 58$. On Figure 4, the number of iterations required for convergence is represented as a function of the amplitude of the perturbation for the two test cases. The calculation was performed 100 times with different random draws to obtain average values. It can be seen that the number of iterations required for convergence

decreases with the amplitude of the perturbation as expected. From $\bar{\nu} = 10^{-2}$, the decrease in the number of iterations is ensured compared to the constant initialization for the two test cases.

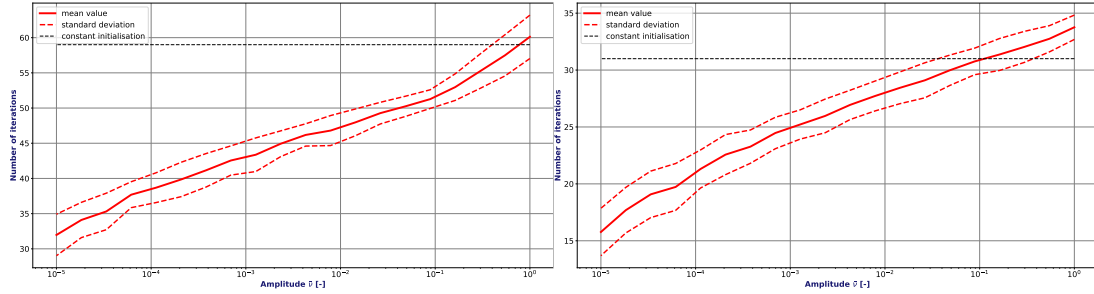


FIGURE 4. Number of iterations before convergence as a function of the perturbation amplitude at initialization (100 random calculations averaged) for the test case (1) (left) and the test case (2) (right).

7. OPTIMIZATION OF THE INITIAL STATE BY MACHINE LEARNING

We propose in this section a prediction technique for the stationary solution using machine learning tools based on neural networks. The classic approach is as follows:

- first, a database containing sets of input parameters $(q_{in}, \theta_{in}, \phi, p_{out})$ and corresponding numerical stationary solutions is obtained using the ThermoTorch code with a constant initialization.
- this database is then used to train a neural network to predict the numerical stationary solution from any input parameters.
- the network is then used to initialize the code in order to decrease the number of iterations required to reach the stationary state.

In order to evaluate the benefits of this approach, we consider a very simplified framework:

- the mesh size is fixed to $N = 50$ cells.
- The homogeneous model with 3 equations, without relative velocity $u_r = 0$, is always considered.

The neural network is programmed using the PyTorch library¹. Based on proposals made in the literature [13,14,17] and after some testing, we have chosen the following features for the network architecture:

- Dense linear neural network with 4 layers, including two hidden layers. The four layers have sizes of respectively 4 (input parameters), 200, 200 and 150 (output values since 3 quantities (p, s, q) need to be predicted for 50 cells, the inner cells of the domain).
- Activation functions are of type ReLU.
- The cost function is of type least squares (MSELoss in PyTorch). The minimization algorithm is the Adam gradient algorithm with default parameters of PyTorch (version 1.13.1). The initial learning rate is set to 0.001.

To train this network, we generated a dataset with 10000 simulation results from ThermoTorch. To do this, we first generated 10000 quadruplets of parameters $(q_{in}, \theta_{in}, \phi, p_{out})$ in the hypercube $[1000, 5000] \times [553.15, 593.15] \times [1 \times 10^7, 5 \times 10^8] \times [140, 170]$ using low discrepancy pseudo-random sequences. Constraints are added to the generation to always consider a liquid flow at the entrance that never fully vaporizes in the medium. The temperature is therefore limited to the saturation temperature (at the output pressure considered) and the heat flow is limited to the total vaporization flow (determined from the other boundary conditions). For each of these parameter sets, the

¹<https://pytorch.org/>

steady-state solution is calculated using the ThermoTorch code. The parameters and dataset are normalized, then used for network training. The network is trained on the dataset with batches of size 50 and over 2000 "epochs" to reach the convergence of the loss. This convergence is illustrated in Figure 5 which represents the loss as a function of the epoch.

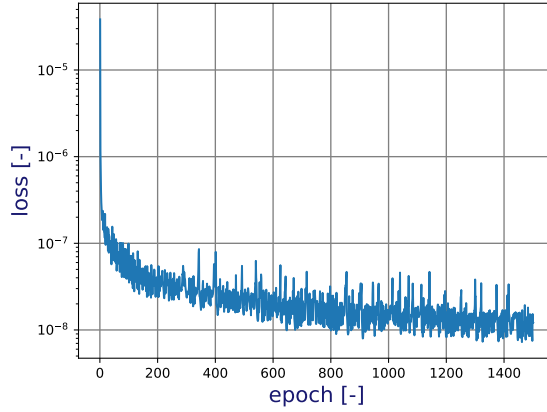


FIGURE 5. Loss function as a function of the epoch.

On Figures 6 (respectively 7), we compare the steady-state solution (calculated with ThermoTorch) with the solution predicted with the neural network for case (1) (respectively case (2)) whose parameters are indicated in table 1. The neural network succeeds in predicting the solution relatively well.

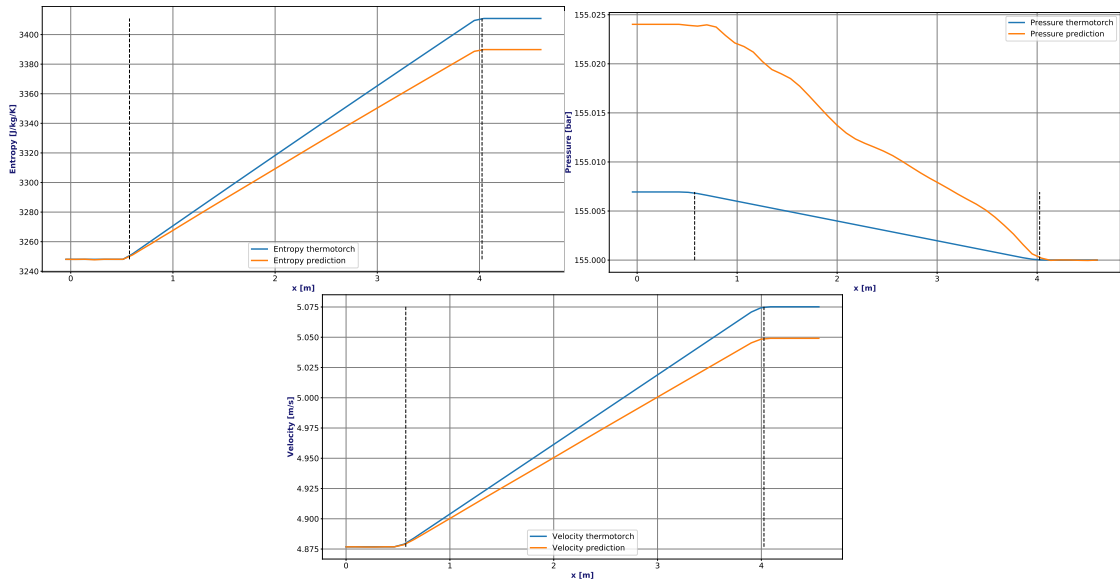


FIGURE 6. Comparison between the ThermoTorch stationary solution and the prediction by neural network for case (1) - $(q_{in}, \theta_{in}, \phi, p_{out}) = (3500 \text{ kg/s}, 320^\circ\text{C}, 10^8 \text{ J/s/m}^3, 155 \text{ bar})$.

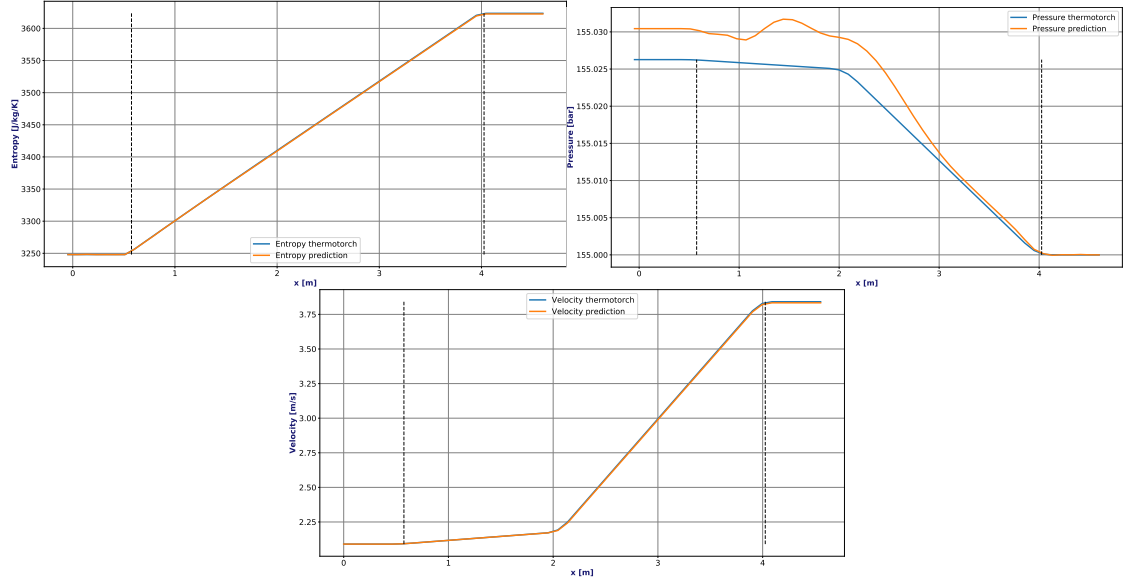


FIGURE 7. Comparison between the ThermoTorch stationary solution and the prediction by neural network for case (2) - $(q_{in}, \theta_{in}, \phi, p_{out}) = (1500 \text{ kg/s}, 320^\circ\text{C}, 10^8 \text{ J/s/m}^3, 155 \text{ bar})$.

We now evaluate the gain of this approach to accelerate the convergence to the steady-state. On a new database of parameters of size 1000, we evaluated the number of iterations before convergence for an initialization with the prediction of the neural network and a constant initialization to compare the two values. We observe in Figure 8 a gain of $21.6 \pm 6.7\%$ in the number of iterations $g_{it} = \frac{N_{it}^{ic} - N_{it}^{ML}}{N_{it}^{ic}}$, and this despite the simplicity of the neural network used. Figure 9 represents the distribution of cases according to the maximum amplitude $\max_x [\nu_{s,p}(x)]$ of the error committed by the prediction with respect to the stationary entropy and pressure fields. It can be noted that this precision could potentially be improved with a better neural network.

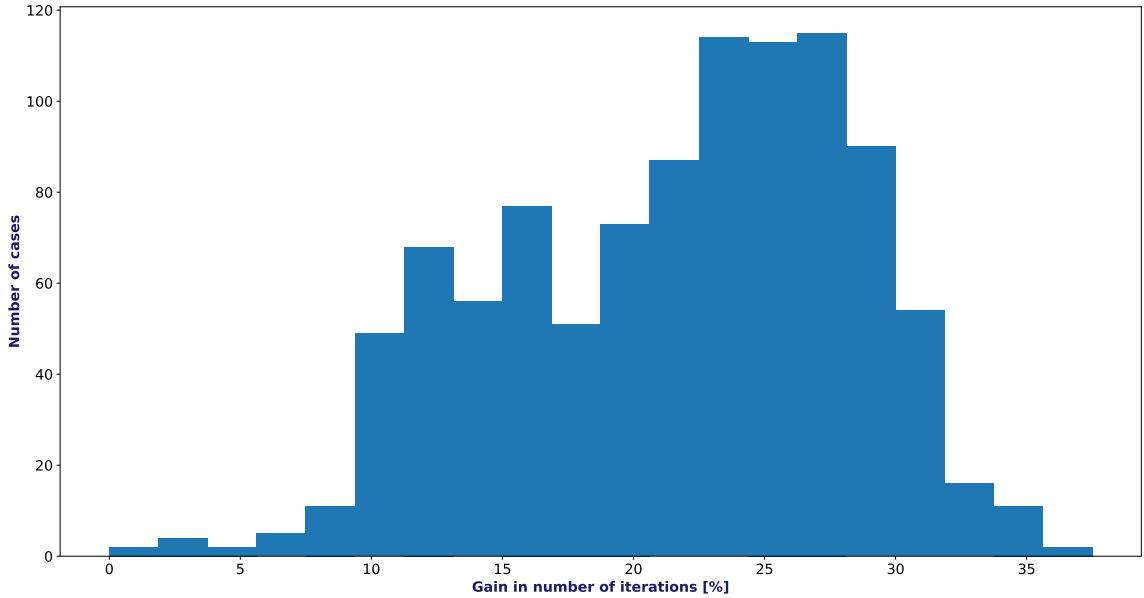


FIGURE 8. Distribution of the number of cases by relative gain in number of iterations on a test base of 1000 cases.

In addition to reducing the number of iterations, the neural network allows for the prediction of states close to the stationary solution, resulting in less oscillations of the fields at convergence.

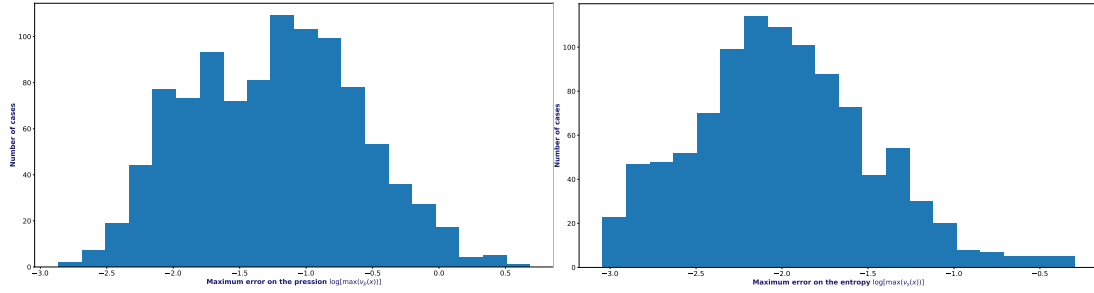


FIGURE 9. Distribution of the maximum error on pressure and entropy on a test base of 1000 cases.

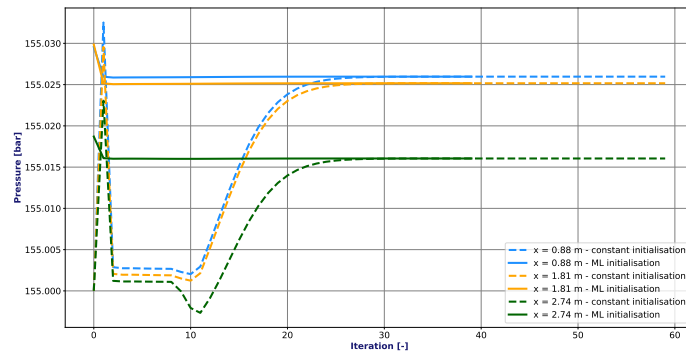


FIGURE 10. Evolution of pressure at 3 points of the mesh ($x_1 = 0.88m$; $x_2 = 1.81m$; $x_3 = 2.74m$) over time for test case (1).

This effect can be observed in Figure 10, which shows the pressure at 3 points of the mesh ($x_1 = 0.88m$; $x_2 = 1.81m$; $x_3 = 2.74m$) over time for case (1). The case with constant initialization is represented by dashed lines, while the case with predicted initialization is represented by solid lines. This could potentially allow for an increase in time step and/or avoid exploration of unstable physical domains during convergence.

8. CONCLUSION

In this work, we have presented a 1D simplified model of a compressible two-phase thermohydraulic flow with phase change. This model is numerically resolved by a semi-implicit scheme in (entropy, pressure-flow rate). The formulation of the numerical scheme allows for the separate resolution of the entropy equation from the other unknowns, which accelerates the algorithm. The scheme is written on a staggered grid to ensure good precision in the low Mach limit.

To accelerate numerical convergence to the stationary state, we have conducted preliminary tests on a machine learning-based initialization method.

The initial results on a very simplified model (homogeneous model with 3 equations, without relative velocity) are promising with a first proposed neural network. Our perspectives are to improve the neural network for more precise predictions and to increase the complexity of the physical model (non-zero relative velocity, addition of the energy equation to account for unsaturated evaporation) to validate this acceleration method on a wider range of cases and in higher dimensions.

9. APPENDIX

9.1. Annexe 1: thermodynamic state law

In this annex, we detail the practical calculation of the coefficients of the thermodynamic laws. For each phase (vapor and liquid), a stiffened gas entropy is used

$$s(\tau, e) = s_0 + c_v \ln \left(\left(\frac{e - h_0 - p_\infty \tau}{\tau^{\gamma-1}} \right) \right).$$

The parameters $(\gamma, c_v, p_\infty, h_0, s_0)$ are unknown for the moment. There are therefore 10 parameters (5 per phase) to choose to establish the complete thermodynamic model. It is impossible to build a precise model over a wide range of temperatures and pressures. It is necessary to settle for a domain in the vicinity of the operating regime of the power plant, i.e. $\theta \simeq 310^\circ C$ and $p \simeq 155$ bar. Calculations (which are detailed, for example, in [2]) allow for the determination of the temperature

$$c_v \theta = e - h_0 - p_\infty a u,$$

the pressure

$$p = (\gamma - 1) \rho c_v \theta - p_\infty,$$

and the enthalpy

$$h = h_0 + \gamma c_v \theta = h_0 + c_p \theta.$$

Consequently, in this model the thermal capacity at constant volume c_v and the thermal capacity at constant pressure c_p are related by

$$c_p = \gamma c_v.$$

The speed of sound is given by

$$c_s^2 = \gamma(p + p_\infty) / \rho.$$

It is then possible to calculate the chemical potential

$$\mu(p, \theta) = h - \theta s.$$

This expression defines the saturation temperature $\theta_s(p)$, which is given by

$$\mu_v(p, \theta_s(p)) = \mu_l(p, \theta_s(p)). \quad (29)$$

9.1.1. Calculation of the coefficients

The International Association for the Properties of Water and Steam (IAPWS) ² proposes precise numerical formulations of the laws of behavior of liquid or steam water. These formulations described in [19] are considered as a reference for establishing other simpler behavior laws. There are Python packages ³ that implement these formulations and allow for the numerical fitting of the coefficients.

Two points (a) and (b) at different temperatures and pressure $p = 155$ bar are considered:

- Point (a) at temperature $\theta_l = 310^\circ C$ to calibrate the liquid properties.
- Point (b) at temperature $\theta_g = 350^\circ C$ to calibrate the vapor properties.

We consider the following pressures and temperatures

$$p^{(a)} = p^{(b)} = 155 \text{ bar}, \quad \theta^{(a)} = 310^\circ C, \quad \theta^{(b)} = 350^\circ C.$$

Furthermore, to fix the derivative of the saturation temperature, we will need the pressure at point (c) :

$$p^{(c)} = 150 \text{ bar}.$$

²<http://www.iapws.org/>

³see for example <https://pypi.org/project/iapws/>

Parameter	Liquid	Vapor	Unit
p_∞	433027888.73886645	2265618.76	Pa
γ	1.347721005	1.092548	-
c_v	3030.1475144213396	3273.937158624049	J/kg/K
h_0	-987900.1770384915	377353.1095	J/kg
s_0	-33462.74606510723	-41040.96603	J/kg/K

TABLE 2. Parameters obtained for the ideal gas laws (liquid and vapor phases).

Liquid water. The parameters to be defined are $\gamma_l, c_{v,l}, p_{\infty,l}, h_{0,l}, s_{0,l}$. The following relationships are used:

- The parameters $(\gamma_l, p_{\infty,l})$ are chosen to impose the speed of sound $c_s^{(a)}$ and the density $\rho^{(a)}$ at point (a), which gives

$$p_{\infty,l} = \frac{\rho^{(a)}(c_s^{(a)})^2}{\gamma_l} - p^{(a)}, \quad \gamma_l = 1 + \frac{p_{\infty,l}}{\rho^{(a)}c_v^{(a)}\theta^{(a)}}.$$

- The heat capacity is fixed to $c_{v,l} = c_v^{(a)}$.
- The reference enthalpy is $h_{0,l} = h^{(a)} - \gamma_l c_{v,l} \theta^{(a)}$.
- The reference entropy $s_{0,l} = s^{(a)} - c_{v,l} \ln\left(\frac{p^{(a)} + p_{\infty,l}}{\gamma_l - 1} \cdot (\rho^{(a)})^{-\gamma_l}\right)$.

Water vapor. The parameters to be defined are $\gamma_v, c_{v,g}, p_{\infty,g}, h_{0,g}, s_{0,g}$. The following relationships are used:

- The parameters $(\gamma_v, p_{\infty,v})$ are chosen to impose the speed of sound $c_s^{(b)}$ and the volume mass $\rho^{(b)}$ at point (b), which gives

$$p_{\infty,v} = \frac{\rho^{(b)}(c_s^{(b)})^2}{\gamma_v} - p^{(b)}, \quad \gamma_v = 1 + \frac{p_{\infty,v}}{\rho^{(b)}c_v^{(b)}\theta^{(b)}}.$$

- The specific heat capacity is set to $c_{v,l} = c_v^{(a)}$.
- Contrary to the liquid case, the reference enthalpies and entropy $s_{0,v}$ and $h_{0,v}$ are calculated to match certain points of the saturation curve $\theta_s(p)$ defined by (29). Specifically, we impose

$$\theta_s(p^{(a)}) = \theta_s^{(a)}, \quad \theta_s(p^{(c)}) = \theta_s^{(c)}.$$

The numerical parameters are detailed in Table 1.

9.1.2. Coefficient of the linearization of the density

To obtain the pressure equation from the mass continuity equation, the linearization (21) is used. The coefficients of this linearization are described below. These coefficients use the derivatives of the density of each phase with respect to the pressure or entropy of that same phase. These derivatives are obtained using the equation of state for each phase as

$$\left(\frac{\partial \rho_k}{\partial p}\right)_{s_k} = \frac{\rho_k}{\gamma_k(p + p_{\infty,k})},$$

$$\left(\frac{\partial \rho_k}{\partial s_k}\right)_p = -\frac{\rho_k}{\gamma_k c_{v,k}}.$$

These formulas also use the total derivative of the vapor entropy with respect to pressure, which is obtained from pressure and saturation temperature as

$$\frac{ds_v}{dp} = c_{v,v} \left(\frac{\gamma_v}{\theta_{sat}(p)} \frac{d\theta_{sat}}{dp}(p) - \frac{\gamma_v - 1}{p + p_{\infty,v}} \right)$$

Coefficient $1/c^2$:

$$\frac{1}{c_s^2} = \rho^2 \cdot \left[\frac{y}{\rho_v^2} \left(\left(\frac{\partial \rho_v}{\partial p} \right)_{s_v} + \left(\frac{\partial \rho_v}{\partial s_v} \right)_p \cdot \frac{ds_v}{dp} \right) + \frac{1-y}{\rho_l^2} \left(\left(\frac{\partial \rho_l}{\partial p} \right)_{s_l} + \left(\frac{\partial \rho_l}{\partial s_l} \right)_p \cdot \frac{y}{1-y} \cdot \frac{ds_g}{dp} \right) \right].$$

Coefficient β :

$$\beta = \frac{\rho^2}{\rho_l^2} \left(\frac{\partial \rho_l}{\partial s_l} \right)_p.$$

Coefficient γ :

$$\gamma = \rho^2 \left(\tau_l - \tau_v + \frac{s_l - s_v}{\rho_l^2} \left(\frac{\partial \rho_l}{\partial s_l} \right)_p \right).$$

REFERENCES

- [1] Melvin R Baer and Jace W Nunziato. A two-phase mixture theory for the deflagration-to-detonation transition (ddt) in reactive granular materials. *International journal of multiphase flow*, 12(6):861–889, 1986.
- [2] Thomas Barberon and Philippe Helluy. Finite volume simulation of cavitating flows. *Computers & fluids*, 34(7):832–858, 2005.
- [3] Herbert B Callen. *Thermodynamics and an Introduction to Thermostatistics*. John Wiley & Sons, 1991.
- [4] Paul Coddington and Rafael Macian. A study of the performance of void fraction correlations used in the context of drift-flux two-phase flow models. *Nuclear Engineering and Design*, 215(3):199–216, 2002.
- [5] Thierry Gallouët, Philippe Helluy, Jean-Marc Hérard, and Julien Nussbaum. Hyperbolic relaxation models for granular flows. *ESAIM: Mathematical Modelling and Numerical Analysis*, 44(2):371–400, 2010.
- [6] Thierry Gallouët, Jean-Marc Hérard, and Nicolas Seguin. Numerical modeling of two-phase flows using the two-fluid two-pressure approach. *Mathematical Models and Methods in Applied Sciences*, 14(05):663–700, 2004.
- [7] Philippe Helluy and Hélène Mathis. Pressure laws and fast legendre transform. *Mathematical Models and Methods in Applied Sciences*, 21(04):745–775, 2011.
- [8] Philippe Helluy and Nicolas Seguin. Relaxation models of phase transition flows. *ESAIM: Mathematical Modelling and Numerical Analysis-Modélisation Mathématique et Analyse Numérique*, 40(2):331–352, 2006.
- [9] Raphaële Herbin, J-C Latché, and Khaled Saleh. Low mach number limit of some staggered schemes for compressible barotropic flows. *Mathematics of Computation*, 90(329):1039–1087, 2021.
- [10] Olivier Hurisse. Numerical simulations of steady and unsteady two-phase flows using a homogeneous model. *Computers & Fluids*, 152:88–103, 2017.
- [11] Olivier Hurisse and Lucie Quibel. Simulations of water-vapor two-phase flows with non-condensable gas using a noble-able-chemkin stiffened gas equation of state. *Computers & Fluids*, 239:105399, 2022.
- [12] Mamoru Ishii and Takashi Hibiki. *Thermo-fluid dynamics of two-phase flow*. Springer Science & Business Media, 2010.
- [13] Siddhartha Mishra. A machine learning framework for data driven acceleration of computations of differential equations. *arXiv preprint arXiv:1807.09519*, 2018.
- [14] Octavi Obiols-Sales, Abhinav Vishnu, Nicholas Malaya, and Aparna Chandramowliswharan. Cfdnet: A deep learning-based accelerator for fluid simulations. In *Proceedings of the 34th ACM international conference on supercomputing*, pages 1–12, 2020.
- [15] Olivier Pironneau. Méthodes des éléments finis pour les fluides. *Masson*, 1988.
- [16] Richard Saurel and Rémi Abgrall. A multiphase godunov method for compressible multifluid and multiphase flows. *Journal of Computational Physics*, 150(2):425–467, 1999.
- [17] Vinicius LS Silva, Pablo Salinas, Matthew D Jackson, and Christopher C Pain. Machine learning acceleration for nonlinear solvers applied to multiphase porous media flow. *Computer Methods in Applied Mechanics and Engineering*, 384:113989, 2021.
- [18] Jean Olive Sylvie Aubry, Christian Caremoli and Paul Rasche. The thyc three-dimensional thermal-hydraulic code for rod bundles: Recent developments and validation tests. *Nuclear Technology*, 112(3):331–345, 1995.
- [19] Wolfgang Wagner and Hans-Joachim Kretzschmar. Iapws industrial formulation 1997 for the thermodynamic properties of water and steam. *International steam tables: properties of water and steam based on the industrial formulation IAPWS-IF97*, pages 7–150, 2008.